Bioorganic Chemistry 165 (2025) 109039

Contents lists available at ScienceDirect

Bioorganic Chemistry

journal homepage: www.elsevier.com/locate/bioorg

Molecular and biological characterization of VEGF-mimetic peptidomimetic containing a morpholine β-amino acid

Raffaella Bucci [a], Lucia De Rosa [b], Gianmarco Bertoni [c], Rossella Di Stasi [b], Maria della Valle [d], Donatella Diana [b], Silvia Peppicelli [c], Kaliroi Peqini [a], Maria Luisa Gelmi [a], Francesca Bianchini [c,*], Luca Domenico D'Andrea [e,*]

[a] Dipartimento di Scienze Farmaceutiche, Università Degli Studi Di Milano, via Venezian 21, 20133 Milano, Italy
[b] Istituto di Biostrutture e Bioimmagini, Consiglio Nazionale delle Ricerche, Via P. Castellino 111, 80131 Napoli, Italy
[c] Dipartimento di Scienze Biomediche Sperimentali e Cliniche "Mario Serio", Università degli Studi di Firenze, Viale G.B. Morgagni 50, 50134 Firenze, Italy
[d] Istituto di Cristallografia, Consiglio Nazionale delle Ricerche, Via Vivaldi 43, 81100 Caserta, Italy
[e] Istituto di Scienze e Tecnologie Chimiche "G. Natta", Consiglio Nazionale delle Ricerche, Via M. Bianco 9, 20131 Milano, Italy

ARTICLE INFO

Keywords:
VEGF
Helical peptide
NMR
Morpholine β-amino acid
Angiogenesis
Endothelial cells

ABSTRACT

The QK peptide is a 15-residue VEGF-mimetic compound known for its proangiogenic activity. Its helical conformation plays a crucial role in binding to VEGF receptors, activating intracellular signaling pathways in endothelial cells, promoting cell migration, proliferation, and survival. However, peptides composed exclusively by natural amino acids often suffer from poor stability in biological fluids, limiting their therapeutic potential. In this study, we modified the QK sequence shortening the peptide chain by incorporating a non-natural β-amino acid with a morpholine core, that promotes helical secondary structures in model peptides. Structural analysis using CD, FT-IR and NMR revealed that in water, MQK adopts a mixed conformation with partial helical content. Biological characterization on endothelial cells demonstrated that MQK peptidomimetic promotes cell proliferation, survival, migration and invasion providing strong evidence for its pro-angiogenic activity, and a reasonable protease resistance. In definitive, insertion of the morpholine β-amino acid partially destabilizes the helical structure and increases peptide flexibility relative to QK, without impairing biological function. This suggests that the enhanced conformational adaptability of MQK may favor adoption of the bioactive conformation and the interaction with the biological target.

1. Introduction

Peptides are a valuable class of molecules for the selective targeting of proteins of interest, as they can establish extensive networks of intermolecular interactions and recognizing large protein surfaces [1]. However, peptides constituted exclusively of natural amino acids are typically unstable in biological fluids, which limits their therapeutic applicability. A well-established strategy to overcome this limitation involves performing structure–function studies to guide the introduction of unnatural amino acids, ultimately evolving the native peptide into a more stable peptidomimetic [2].

The QK peptide (Ac-KTLWQELYQLKYKGI-amide) is a 15-mer VEGF-mimetic compound with proangiogenic activity [3,4]. It consists entirely of natural amino acids and adopts a helical structure that is essential for its biological function. The QK peptide reproduces the α1 helix of VEGF (residues from 17 to 25), binds to VEGF receptors [5] and activates intracellular pathways in endothelial cells, ultimately promoting cell migration, proliferation and survival [6]. In vivo studies have demonstrated that QK can recapitulate VEGF's biological properties in various experimental models [7–10]. In recent years, biomaterials decorated with QK peptide have been reported for applications in tissue regeneration [11].

In the last years, we reported a few attempts to modify QK sequence to improve its structural stability with unnatural amino acids without compromising its biological activity. We showed that Leu10, a residue critical for the peptide folding and stability [12], can be replaced with norleucine maintaining the peptide helical conformation and biological activity [13]. Then, we focused on the N-terminal region (Lys1-Thr2-Leu3), which was designed to stabilize the helix conformation by acting as N-capping motif [14]. Molecular dynamics simulations and peptide

* Corresponding authors.
E-mail addresses: francesca.bianchini@unifi.it (F. Bianchini), luca.dandrea@cnr.it (L.D. D'Andrea).

https://doi.org/10.1016/j.bioorg.2025.109039
Received 11 July 2025; Received in revised form 25 September 2025; Accepted 26 September 2025
Available online 27 September 2025

deletion studies confirmed that this region effectively stabilizes the helix and nucleates helical formation [12]. Although not directly involved in receptor recognition [5], deletion of this N-terminal segment was shown to markedly reduce peptide activity, primarily due to decreased helical population [15]. Interestingly, chiral inversion of the first three residues (D-Lys1, D-Thr2, D-Leu3) destabilized the initial helical turn but only modestly impaired biological activity [16]. Furthermore, NMR analysis of QK peptide in water revealed that the N-terminal region is frayed, as expected for termini of short peptides [3]. This conformational flexibility contributes to increased protease susceptibility [17].

To fully exploit the therapeutic potential of the natural sequence, in this study we converted QK into a peptidomimetic by introducing unnatural amino acid. This idea is based on the well-known increased stability of peptidomimetics compared to natural peptides in proteolytic environments. Additionally, incorporating a conformationally constrained non-natural amino acid may influence the overall structure of the sequence, thereby enhancing its stability [18,19]. Specifically, we exploited the replacement of the QK N-terminal region with a molecular scaffold designed to promote helix formation while minimizing terminal fraying. We focused on the morpholine β-amino acid (hereafter referred to as Morph), a γ-turn inducer [20], which can form hydrogen bonds with the amide protons of the *i*+1 and *i*+2 residues (in some case also *i*+3) suggesting its role as a N-capping residue. Furthermore, molecular dynamics studies of the model peptide sequence Boc-(Morph-Leu-Val)$_2$-OBn revealed that this scaffold supports conformations compatible with α-helical and/or polyproline II structures, in agreement with NMR findings [18,20,21].

The combined properties of Morph, as potential turn inducer by formation of one/two hydrogen bond(s) with residues in the first helical turn, prompted us to incorporate it into QK, shortening the sequence, with the aim to improve proteolytic and conformational stability, ensuring its biological function.

2. Results and discussion

2.1. Peptide synthesis and analytical characterization

The MQK peptide (AcMorph-WQELYQLKYKGI-amide) was prepared by solid phase peptide synthesis using the Rink-Amide ChemMatrix resin coupling the acetyl-Morph residue, which was acetylated slightly modifying the synthetic procedure already reported [20], to the peptidyl-resin. Analytical and spectroscopic spectra of acetyl-Morph and its alcohol are reported in the SI (Fig. S1-S5). After resin cleavage, the peptide was purified by RP-HPLC and identified by HR-MS (Fig. S6).

2.2. Structural characterization

2.2.1. Circular dichroism (CD) spectroscopy

MQK was analyzed at 100 μM in potassium phosphate (5 mM) buffer at pH 7.0, and in presence of increasing amount of trifluoroethanol (TFE). The CD spectrum in phosphate buffer (Fig. 1) shows the presence of a minimum around 203 nm and a less pronounced minimum around 220 nm. Under 200 nm the CD signal becomes positive, but a maximum is not evident. This analysis suggests that MQK peptidomimetic in phosphate buffer assumes a mixture between helix and unordered conformations (prevalent). However, in the presence of increasing concentration of TFE (Fig. 1) we observed the CD signature of a helix conformation, with a shift of the minimum towards 207 nm, the increase of the intensity of the minimum at 222 nm and the formation of a positive maximum at 193 nm. The crossover point shifts from 193 nm to 201 nm. Furthermore, an isodichroic point is evident at 203 nm indicating the equilibrium between the helix and unordered conformations. The helix formation is almost complete already at 20% TFE. Overall, the CD analysis suggests that MQK peptidomimetic scarcely populated the helix conformation in aqueous buffer, but it has a good propensity to adopt the helical conformation as happens in presence of TFE.

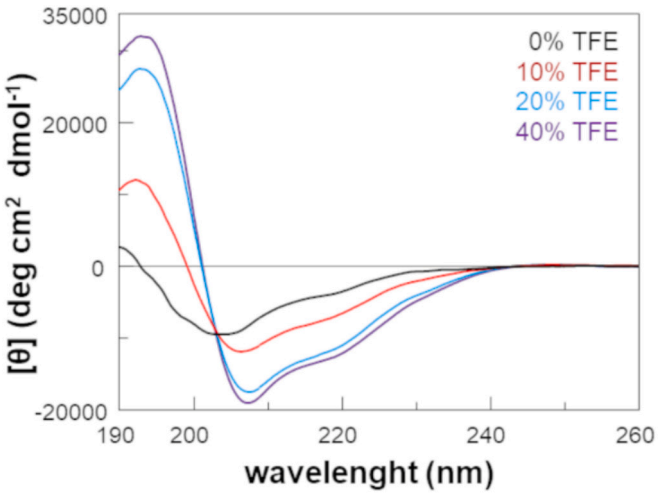

Fig. 1. Circular dichroism analysis. Far-UV CD spectra of MQK in 5 mM potassium phosphate buffer, pH 7.0 with increasing concentration of trifluoroethanol (TFE). Spectra were acquired at 20 °C and reported as mean residue ellipticity [θ].

2.2.2. ATR-FTIR spectroscopy

QK and MQK peptides were analyzed in the solid state. Fig. 2 shows the comparison between QK and its analogue MQK.

The deconvolution of the amide I band indicated two peaks for both peptides. The peak centered at 1623 cm^{-1} was attributed to an extended conformation, while the peak at 1656 cm^{-1} is indicative of a helical structure [22]. FT-IR analysis demonstrated that both peptides adopt a mixture of two conformations in the solid state. The QK peptide exhibits approximately the 15% of extended conformation and 85% α-helical structure (Fig. 2A), whereas MQK (Fig. 2B) is mainly present as an extended conformation (about 60%) with the remaining 40% as helix conformation.

2.2.3. NMR spectroscopy

To investigate the conformational properties of the MQK peptidomimetic in solution, we performed a complete NMR characterization (^{1}H NMR [600 MHz], ^{13}C NMR [150 MHz], COSY, TOCSY, NOESY and ROESY experiment; see Supporting Information). An almost complete proton resonance assignment was achieved by analysis of the 2D [^{1}H−^{1}H] TOCSY and the chemical shifts were assigned to each amino acid (Table TS1). 2D [^{1}H—^{1}H] NOESY and ROESY spectra were recorded for giving an insight on the potential helix conformation of MQK peptidomimetic.

The acetyl-morpholino amino acid (AcMorph; Fig. 3A) is present as a mixture of two conformers (Figs. 3B and S7A) corresponding to the two rotamers of the amide bond of the acetyl group. The different proximity of the methyl group to H-3 and H-5 protons of AcMorph is demonstrated by the ROESY experiment (Fig. S8A) and detailed in Fig. 3B. As already reported [20,21], the morpholine oxygen may drive the orientation of the NH of the amino acid at position *i*+1, in our case NH$_{W2}$, through an unusual hydrogen bond. As a result, a γ-turn could be formed, stabilized by a H-bond between C=O$_{Morph}$ and the NH of amino acid at position *i*+2 (i.e. NH$_{Q3}$). Unfortunately, since the H-6$_{Morph}$/H$_{αW2}$ resonances are very close (Fig. S8B), we were not able to assign unequivocally the ROE between these two protons, that would be diagnostic for this turn. On the other hand, the ROE between H$_{αW2}$ and NH$_{Q3}$ (*i*, *i*+1) is unequivocally detected, proving the presence of the above mentioned γ-turn (Figs. 3C and S8C). The presence of H-bonds in this region is suggested by the experiment at variable temperature (Table TS2; from 298 to 253 K). The Δδ/ΔT ratio is about 4.4 and 5 ppb for NH$_{W2}$ and NH$_{Q3}$, respectively. These relatively large values could be explained by the presence of the two rotamers that are in equilibrium. This could be also

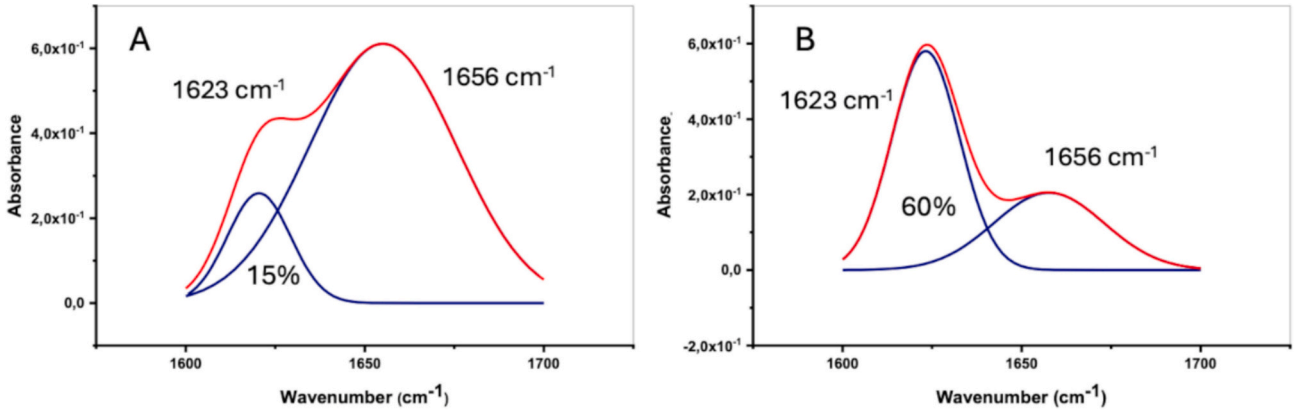

Fig. 2. ATR-FTIR spectroscopy. Deconvolution of the amide I band of QK peptide (A) and MQK peptidomimetic (B).

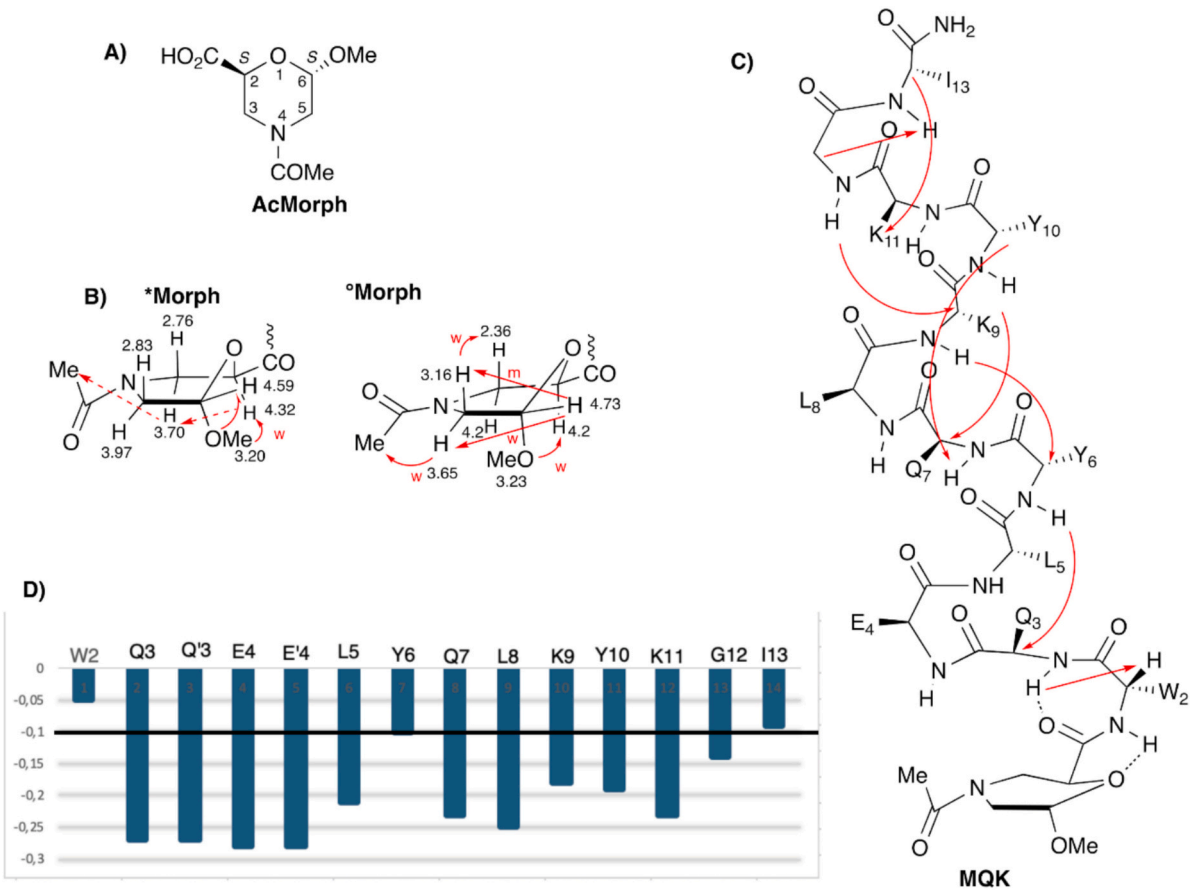

Fig. 3. A) (2S,6S)-4-Acetyl-6-methoxymorpholine-2-carboxylic acid; B) *N*-acetylated rotameric *Morph and °Morph moieties and ROEs (red arrows); C) MQK sequence with the indication of the observed ROEs (red arrows); D) Secondary chemical shifts of Hα (ΔδHα) of the MQK peptidomimetic calculated in water. Solid line indicates the cutoff value for identifying the elements of secondary structure according to Wishart and Sykes [23]. (For interpretation of the references to colour in this figure legend, the reader is referred to the web version of this article.)

the reason why two glutamines (Gln3) and two glutamic acids (Glu4) were detected in a very close proximity (Fig. S7B).

Comparing the observed H_α chemical shift values for MQK with the ones reported in literature for random coil conformations [23] ($\Delta\delta H_\alpha$ values, Fig. 3D), we observe consecutive lower values then −0.1 except for Trp2, involved in the γ-turn, and Ile13 at C-terminus. According to the literature [24] this behavior suggests a helical conformation (Fig. 3C).

Our hypothesis is also supported by ROESY experiments. However, it was impossible to detect ROEs between NH/NH (*i, i*+1) due to the close chemical shifts of most consecutive protons. On the contrary, all H_α/NH (*i, i*+1) spatial proximities were detected, as well as several H_α/NH (*i, i*+3) that are those of $H_{\alpha K9}/NH_{G12}$, $H_{\alpha Q7}/NH_{Y10}$, $H_{\alpha Y6}/NH_{K9}$ and $H_{\alpha Q3}/NH_{Y6}$ (Figs. 3C and S8C). Unfortunately, the close proximity of both H_α and NH chemical shifts of not mentioned amino acids at position *i, i*+3 prevents us to unequivocally assign some ROEs which could not be excluded due to the presence of strong cross peaks in that area.

Other ROEs are those of $H_{\alpha G12}/NH_{I13}$ (*i, i*+1) (Fig. S8C) and $H_{\alpha I13}/H_{\delta K11}$ (Fig. S8D). These spatial proximities are possible due to the presence of the two H_α protons of Gly and the conformational freedom of

Ile13, respectively. An anomalous ROE for a helical conformation was detected and is referred to the spatial proximity between the $H_{\alpha Y10}$ and NH_{Q7} [H_α/NH (*i, i*-3)] (Fig. S8C). The presence of this peculiar signal could not make us exclude the presence of other conformations.

The experiment at variable temperature did not help to support our hypothesis on the presence of a helix construct, due to the close chemical shifts of NH protons, except for isolated NHs that are those of the γ-turn region (see above) and for NH_{G12}, for which a qualitative value of about 3.4 ppb was detectable (Table TS2).

As a matter of fact, the spectroscopic characterization performed on MQK suggests that in water the peptidomimetic slightly adopts an α-helix conformation, and it is mainly present as unordered conformation. However, it has a good propensity to adopt full helical conformation in the presence of specific conditions as revealed by CD experiments.

2.3. Biological characterization

2.3.1. MQK peptidomimetic promotes cell proliferation and survival of HUVEC

To assess the viability of HUVEC cells supported by MQK peptidomimetic, cells were cultured in 2% serum and treated with MQK (10, 25, 50, and 100 ng/mL), QK (10, 25, 50, and 100 ng/mL) or recombinant human Vascular Endothelial Growth Factor A (rhVEGF-A, 25 ng/mL) as controls. Cell viability was determined using a 3-(4,5-dimethylthiazol-2-yl)-2,5-diphenyltetrazolium bromide (MTT) reduction assay at 48 h post-treatment. Interestingly, all peptides exhibited a dose-dependent response. All concentrations of MQK demonstrated an increase in cell viability ranging from 51% to 81% compared to untreated cells ($p <$ 0.0001). Notably, MQK at 50 ng/mL increased viability by 24% compared to QK at the same concentration ($p < 0.001$), and MQK at 100 ng/mL increased viability by 28% compared to QK at the same concentration ($p < 0.0001$) (Fig. 4).

To evaluate whether the MQK peptidomimetic exhibits VEGF-like pro-survival activity, a western blot analysis for the cleaved form of

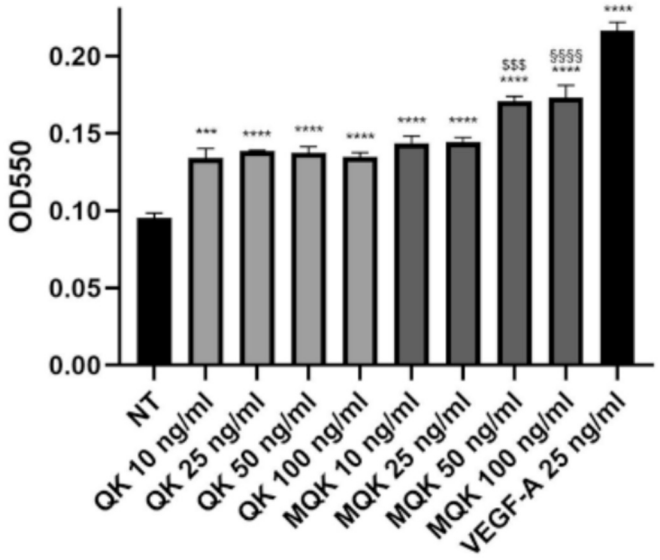

Fig. 4. Evaluation of viability. MTT assays were conducted on HUVEC cells treated with varying concentrations of MQK (10, 25, 50, and 100 ng/mL), QK (10, 25, 50, and 100 ng/mL), or rhVEGF-A (25 ng/mL) serving as controls, for 48 h. Figure shows the most representative result out the three-independent experiments performed. To compare the different groups, a one-way ANOVA was performed. Data are expressed as mean ± SEM. Statistical significance was assumed for *p*-values ≤0.05: * $p < 0.05$ ** $p < 0.01$ *** $p < 0.001$ **** $p <$ 0.0001 vs untreated (NT); # $p < 0.05$ ## $p < 0.01$ vs VEGF-A; $$$ $p < 0.001$ vs QK 50 ng/mL; §§§§ $p < 0.0001$ vs QK 100 ng/mL.

Poly(ADP-ribose) polymerase 1 (PARP-1), was performed on HUVEC cells. The cells were treated for 15 min with MQK (50 ng/mL), QK (50 ng/mL), or rhVEGF-A (50 ng/mL) in 2% serum EBM after 2 h of serum deprivation.

After the treatment, cells exposed to MQK showed a significant decrease in cleaved PARP-1 expression compared to untreated cells, indicating a reduction in caspase-3 expression and in apoptotic activity ($p < 0.0001$) (Fig. 5A). Analogous results were observed in cells treated with QK and rhVEGF-A, demonstrating that MQK has VEGF-like pro-survival effects (Fig. 5B).

To further assess the proliferative effects of the MQK peptidomimetic, a western blot analysis for the phosphorylated form of Extracellular-signal Regulated Kinase 1/2 (pERK1/2) was conducted. HUVEC cells were treated for 15 min with MQK (50 ng/mL), QK (50 ng/mL), or rhVEGF-A (50 ng/mL) in 2% serum EBM after 2 h of serum deprivation.

Cells treated with MQK showed a 41% increase in pERK1/2 expression compared to untreated cells ($p < 0.0001$), indicating enhanced cell proliferation. Similarly, cells treated with QK or rhVEGF-A exhibited increases in pERK1/2 expression ranging from 29% to 53% compared to untreated cells ($p < 0.0001$), confirming the proliferative effects of these treatments (Fig. 5C).

2.3.2. MQK peptidomimetic promoted endothelial cells migration and invasion

The proangiogenic potential of MQK was evaluated using an invasion assay employing a transwell insert coated with a synthetic extracellular matrix (Geltrex). HUVEC cells were cultured on the transwell insert, with medium containing respective treatments added below. MQK was administered at a concentration of 50 ng/mL, while QK and rhVEGF-A were included at identical concentrations as controls. The use of 50 ng/mL concentration in the migration and invasion assays was selected based on previous biological studies [6] with QK and supported by the results of the MTT assay. Following 24 h of treatment, cells were fixed with 4% paraformaldehyde and stained with 0.5% crystal violet.

The results demonstrated that the invasiveness of cells treated with MQK increased by 52% compared to untreated cells ($p < 0.001$), albeit with a decrease of only 27% when compared to rhVEGF-A. Moreover, when compared to QK, the decrease was even less significant, with a value of 6% (Fig. 6).

To support and expand upon the results from the invasion assay, a scratch assay was conducted. This assay measures the migration of adherent cells, which can be correlated with reparative angiogenesis, a critical process in wound healing and revascularization. Reduced areas reflect an increased migratory capacity.

For this experiment, HUVEC cells were treated with 50 ng/mL of MQK, with QK and rhVEGF-A used at the same concentration as controls, for a duration of 6 h. Images were captured at the start of the experiment (T0) and after 6 h (T6) to mark the endpoint of the protocol. The wound area was quantified using QuPath software. The results showed that the wound area for cells treated with MQK was reduced by 35% compared to untreated cells ($p < 0.01$). In comparison, cells treated with QK exhibited a 30% reduction, while those treated with rhVEGF-A demonstrated a 44% reduction in wound area (Fig. 7). These findings highlight the ability of MQK to promote cell migration, thereby enhancing reparative angiogenesis in endothelial cells.

2.3.3 *Effect of MQK peptidomimetic on in vitro tubulogenic ability of endothelial cells*

The tubulogenic assay evaluates the ability of endothelial cells to give rise to a capillary-like network as a measure of regenerative property. This biological characteristic correlates with reparative angiogenesis. For this experiment, HUVEC cells were seeded on a synthetic extracellular matrix and treated with MQK, QK or rhVEGF-A at 50 ng/mL concentration for 24 h. Images were captured at the end of the incubation to quantify the number of nodes in each treatment. Though this induction was not significant, cells treated with MQK and QK weakly

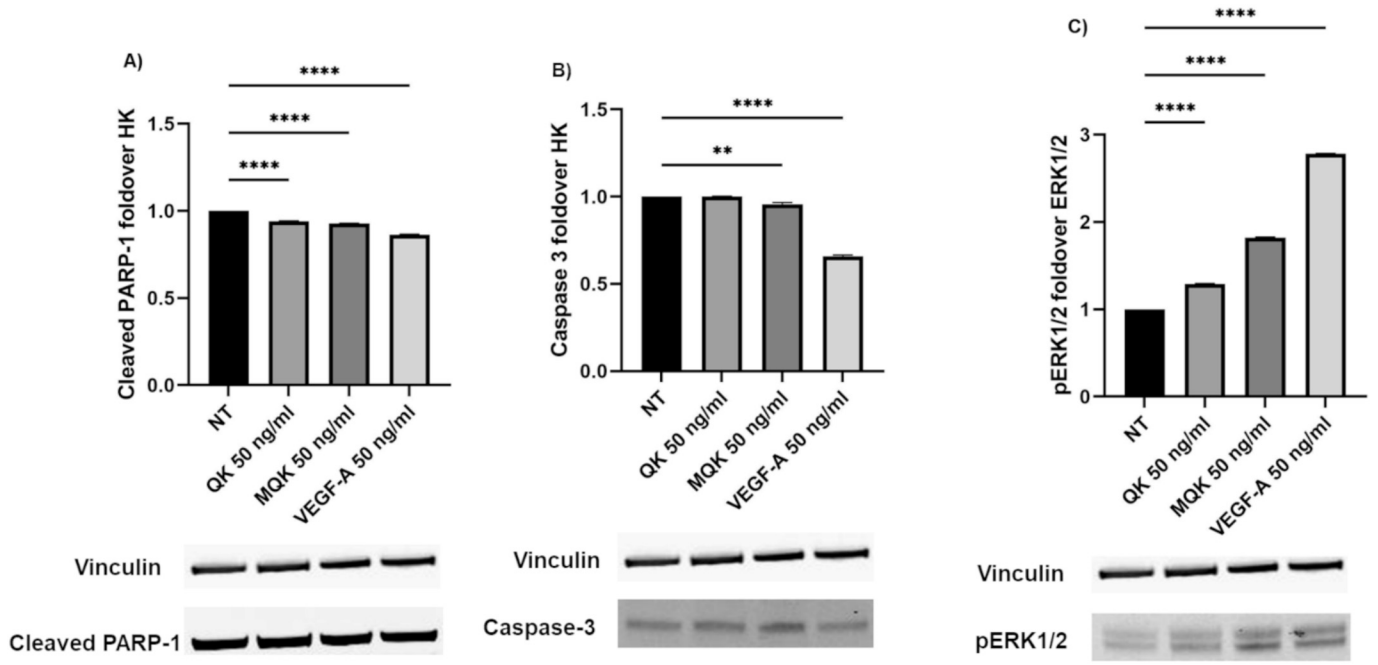

Fig. 5. Assessment of apoptotic activity and proliferation. A western blot assay was conducted on serum-starved HUVEC cells treated for 15 min with 50 ng/mL of MQK, QK, or rhVEGF-A as controls. To evaluate the differences between the samples, a one-way ANOVA test was performed using GraphPad Prism software. Upper panels: densitometric analysis presented as the mean ± SEM of the most representative experiment out of the three independent replicates; lower panels: relative western blot results of the representative experiment. Statistical significance was assumed for *p*-values ≤0.05: ** $p < 0.01$, **** $p < 0.0001$ compared to untreated cells (NT).

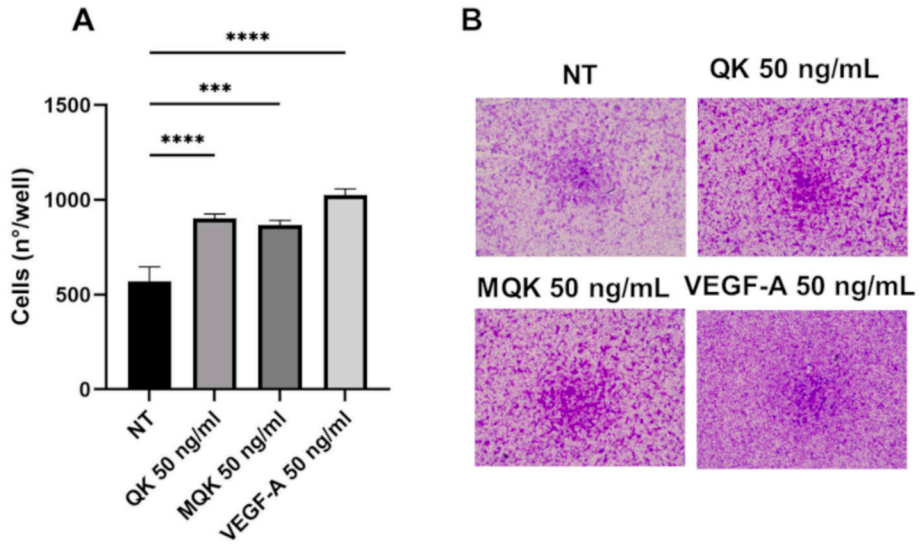

Fig. 6. Evaluation of invasiveness. Invasion assays were conducted on HUVEC cells treated for 24 h with 50 ng/mL of MQK, QK, or rhVEGF-A as controls. A) Quantification of the number of cells migrated through Geltrex-coated filters. Data are presented as mean ± SEM from four 10× images of the most representative experiment. B) Images (4× magnification) from the most representative experiment. To evaluate the differences between the samples, a one-way ANOVA test was performed using GraphPad Prism software. Statistical significance was assumed for *p*-values ≤0.05: ***$p < 0.001$ and **** $p < 0.0001$ compared to untreated cells (NT).

increased their tubulogenic ability, on the other hand, only cells treated with rhVEFG-A showed a significant increase in the number of nodes (Fig. 8).

Our investigation into the biological effects of the MQK peptidomimetic on endothelial cell function and angiogenesis has yielded several significant findings with potential therapeutic implications. The multifaceted actions of MQK, as evidenced by its impact on endothelial cell proliferation, survival, migration, and invasion, underscore its promise as a novel therapeutic agent for promoting tissue repair and regeneration.

One of the key findings of our study is the dose-dependent enhancement of cell viability in HUVEC cultures treated with MQK. Notably, MQK exhibited potent cytoprotective effects, as evidenced by the significant reduction in cleaved PARP-1 expression, indicating attenuated apoptotic activity. These observations highlight the potential of MQK to promote endothelial cell survival under conditions of stress or

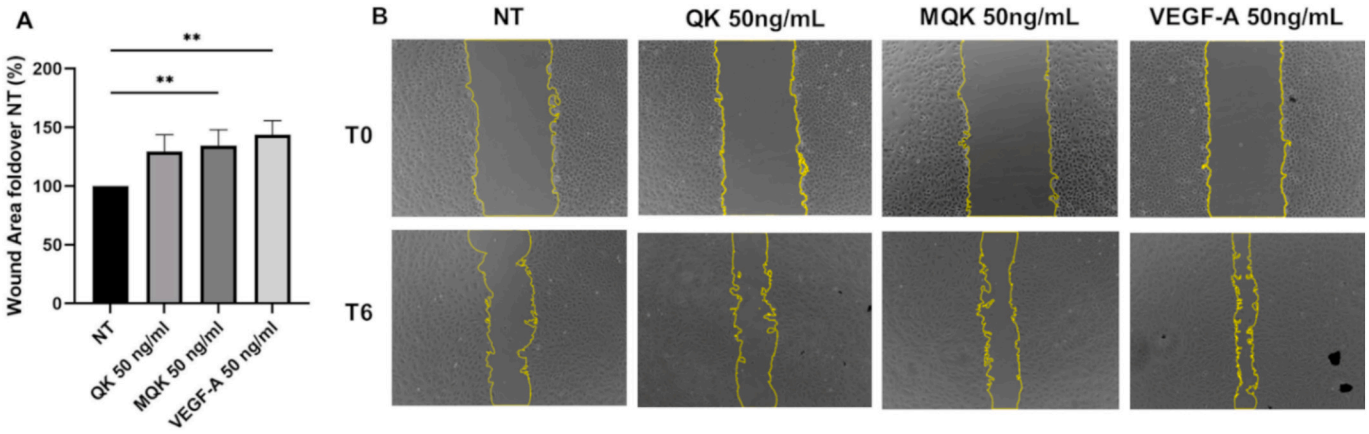

Fig. 7. Evaluation of HUVEC cell migration using a scratch assay. HUVEC cells were treated for 6 h with 50 ng/mL of MQK, QK or rhVEGF-A at the same concentration serving as controls. A) Quantification of HUVEC cells migration. The wound area, measured using QuPath software, is reported as percentage of wound closure compared to untreated cells. GraphPad Prism software was used for statistical analysis, and comparisons among treatments were carried out using a one-way ANOVA test. Data are expressed as mean ± SEM from two independent experiments. Statistical significance was assumed for *p*-values ≤0.05: $*p < 0.05$ compared to untreated cells (NT). B) Representative images of the most representative experiment performed depict the healing process under basal conditions and after stimulation with the treatments. Images were captured at the start (T0) and after 6 h (T6) of the experiment.

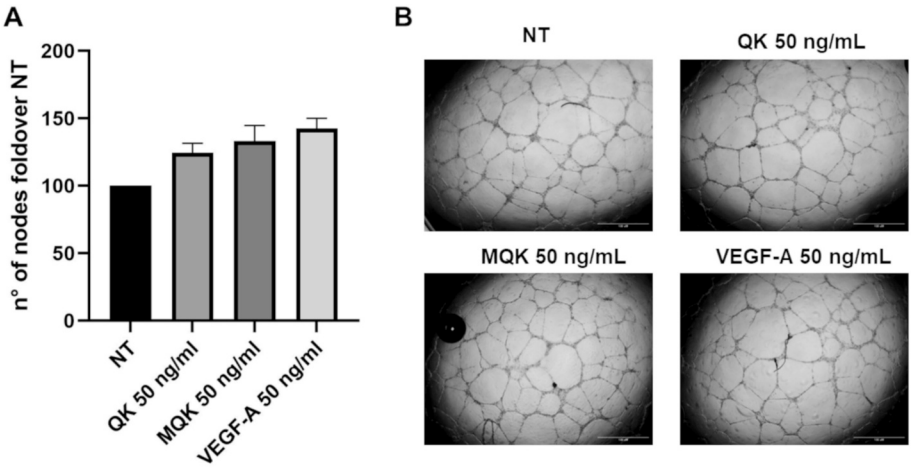

Fig. 8. In vitro tubulogenesis in HUVECs grown for 24 h in the presence of 50 ng/mL of MQK, QK, or rhVEGF-A. A) Quantification of in vitro tubulogenesis expressed as mean value ± SD of the node number. GraphPad Prism software was used for statistical analysis, and comparisons among different treatments vs untreated cells were carried out using a one-way ANOVA test. Statistical significance was assumed for *p*-values ≤0.05: $*p < 0.05$ compared to untreated cells. Experiments were conducted in triplicate. B) Representative images of different treatments.

injury, which is crucial for neovascularization and tissue repair. Specifically, MQK treatment led to a remarkable increase in cell viability after 48 h, with concentrations ranging from 51% to 81% compared to untreated cells.

Moreover, our investigation revealed the proliferative effects of MQK on endothelial cells, as evidenced by the upregulation of phosphorylated ERK1/2 (pERK1/2). The activation of the ERK1/2 pathway by MQK suggests its involvement in promoting cell cycle progression and mitogenic responses, essential for angiogenesis and tissue regeneration. The robust proliferative effects of MQK underscore its potential as a therapeutic agent for enhancing neovascularization in ischemic or injured tissues. Specifically, MQK treatment resulted in a 41% increase in pERK1/2 expression compared to untreated cells.

Furthermore, our study demonstrated the ability of MQK to enhance endothelial cell migration and invasion, critical processes in wound healing and tissue repair. The observed increase in cell migration and invasion following MQK treatment highlights its potential to accelerate wound closure and promote tissue regeneration. Surprisingly, we found that MQK and QK express only a slight and not significant increase in tubulogenic ability compared to untreated cells. Overall, these findings are particularly relevant in clinical settings where impaired angiogenesis contributes to delayed wound healing and compromised tissue repair. Specifically, the invasiveness of cells treated with MQK increased by 52% compared to untreated cells.

Overall, our study provides compelling evidence for the pro-angiogenic effects of the MQK peptidomimetic, highlighting its therapeutic potential for promoting tissue repair and regeneration, particularly in contexts where angiogenesis plays a critical role in physiological and pathological processes.

2.4. MQK stability in human serum

For the pharmacological application of peptides, adequate stability in the human body is essential. A commonly used approach to assess proteolytic stability involves measuring the peptide half-life in human serum. To this end, we performed HPLC analyses of the MQK and QK peptides (Fig. S9) following incubation in 50% human serum at various time points (Fig. 9).

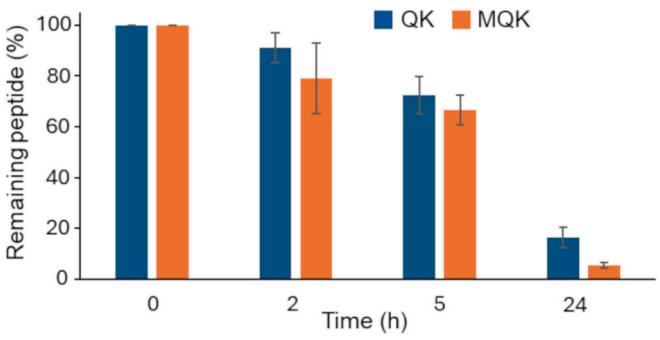

Fig. 9. Analysis of the stability of MQK and QK peptides in 50% human serum. The residual amount of peptide was quantified by RP-HPLC determining the area of the peptide peak revealed at 210 nm at the indicated incubation time. Data is reported as a means of a triplicate experiment.

The MQK peptide exhibits a half-life exceeding 5 h in 50% human serum and is fully metabolized within approximately 24 h. These results indicate a high degree of stability against plasma proteases, considering that peptides are typically degraded within 15–30 min under similar conditions. MQK and QK peptides showed comparable stability, indicating that the primary proteolytic cleavage sites reside within the core sequence rather than at the N-terminus. However, we expect that, upon elimination of these main cleavage sites, e.g. through the incorporation of unnatural amino acids, secondary cleavage sites may become exposed. Under such conditions, the peptide presenting the morpholine scaffold is expected to exhibit enhanced stability compared to the peptide bearing the original peptide sequence (Lys-Thr-Leu).

3. Conclusions

We modified the QK peptide by replacing its N-terminal region with a morpholine β-amino acid scaffold. Structural analysis using CD, FT-IR and NMR revealed that in water, MQK adopts a mixed conformation, mainly unordered, with partial helical content. Biological characterization on endothelial cells demonstrated that MQK promotes cell proliferation, survival, migration and invasion providing strong evidence for its pro-angiogenic activity. Furthermore, MQK exhibits reasonable protease resistance comparable to the parent peptide QK.

In definitive, insertion of the morpholine β-amino acid partially destabilizes the helical structure and increases peptide flexibility relative to QK, without impairing biological function. This suggests that the enhanced conformational adaptability of MQK may favor adoption of the bioactive conformation and the interaction with the biological target (VEGF receptors). Notably, peptides that exhibit different accessible conformational states may be significantly more effective than rigid ones in modulating protein–protein interactions for their adaptability. [25,26].

In conclusion, our findings highlight the potential of the MQK peptidomimetic, analogue of the known QK peptide, as a promising therapeutic candidate for tissue repair and regeneration.

4. Experimental section

Experimental details are reported in the supplementary information.

CRediT authorship contribution statement

Raffaella Bucci: Writing – review & editing, Writing – original draft, Visualization, Investigation. **Lucia De Rosa:** Writing – review & editing, Writing – original draft, Visualization, Investigation. **Gianmarco Bertoni:** Visualization, Investigation. **Rossella Di Stasi:** Resources, Investigation. **Maria della Valle:** Visualization, Investigation. **Donatella Diana:** Writing – review & editing, Supervision. **Silvia Peppicelli:** Writing – original draft. **Kaliroi Peqini:** Investigation. **Maria Luisa Gelmi:** Writing – review & editing, Supervision, Funding acquisition, Conceptualization. **Francesca Bianchini:** Writing – review & editing, Supervision, Funding acquisition. **Luca Domenico D'Andrea:** Writing – review & editing, Supervision, Funding acquisition, Conceptualization.

Funding sources

This work was supported by Ministero dell'Università e della Ricerca (MUR) under the programme PRIN2020 (Cod. 2020833Y75).

Declaration of competing interest

The authors declare that they have no known competing financial interests or personal relationships that could have appeared to influence the work reported in this paper.

Acknowledgments

F.B. thanks the University of Florence for support through the fondo ricerca di ateneo "RICATEN 2020-2023".

Mass spectrometry analyses and NMR analyses were performed using facilities of the Unitech COSPECT at the University of Milan (Italy)".

Appendix A. Supplementary data

Supplementary data to this article can be found online at https://doi.org/10.1016/j.bioorg.2025.109039.

Data availability

Data will be made available on request.

References

[1] L. Nevola, E. Giralt, Modulating protein-protein interactions: the potential of peptides, Chem. Commun. (Camb.) 51 (16) (2015) 3302–3315, https://doi.org/10.1039/c4cc08565e.

[2] R.M. Liskamp, D.T. Rijkers, J.A. Kruijtzer, J. Kemmink, Peptides and proteins as a continuing exciting source of inspiration for peptidomimetics, Chembiochem 12 (11) (2011) 1626–1653, https://doi.org/10.1002/cbic.201000717.

[3] L.D. D'Andrea, G. Iaccarino, R. Fattorusso, D. Sorriento, C. Carannante, D. Capasso, B. Trimarco, C. Pedone, Targeting angiogenesis: structural characterization and biological properties of a de novo engineered VEGF mimicking peptide, P Natl Acad Sci USA 102 (40) (2005) 14215–14220, https://doi.org/10.1073/pnas.0505047102.

[4] R. Di Stasi, L. De Rosa, L.D. D'Andrea, Structure-based Design of Peptides Targeting VEGF/VEGFRs, Pharmaceuticals (Basel) 16 (6) (2023) 851, https://doi.org/10.3390/ph16060851.

[5] R. Di Stasi, D. Diana, D. Capasso, S. Di Gaetano, L. De Rosa, V. Celentano, C. Isernia, R. Fattorusso, L.D. D'Andrea, VEGFR recognition Interface of a proangiogenic VEGF-mimetic peptide determined in vitro and in the presence of endothelial cells by NMR spectroscopy, Chem-Eur J 24 (44) (2018) 11461–11466, https://doi.org/10.1002/chem.201802117.

[6] F. Finetti, A. Basile, D. Capasso, S. Di Gaetano, R. Di Stasi, M. Pascale, C.M. Turco, M. Ziche, L. Morbidelli, L.D. D'Andrea, Functional and pharmacological characterization of a VEGF mimetic peptide on reparative angiogenesis, Biochem. Pharmacol. 84 (3) (2012) 303–311, https://doi.org/10.1016/j.bcp.2012.04.011.

[7] G. Santulli, M. Ciccarelli, G. Palumbo, A. Campanile, G. Galasso, B. Ziaco, G. G. Altobelli, V. Cimini, F. Piscione, L.D. D'Andrea, C. Pedone, B. Trimarco, G. Iaccarino, In vivo properties of the proangiogenic peptide QK, J. Transl. Med. 7 (2009) 41, https://doi.org/10.1186/1479-5876-7-41.

[8] G.K. Dudar, L.D. D'Andrea, R. Di Stasi, C. Pedone, J.L. Wallace, A vascular endothelial growth factor mimetic accelerates gastric ulcer healing in an iNOS-dependent manner, Am. J. Physiol. Gastrointest. Liver Physiol. 295 (2) (2008) G374–G381, https://doi.org/10.1152/ajpgi.90325.2008.

[9] A. Verheyen, E. Peeraer, D. Lambrechts, K. Poesen, P. Carmeliet, M. Shibuya, I. Pintelon, J.P. Timmermans, R. Nuydens, T. Meert, Therapeutic potential of VEGF and VEGF-derived peptide in peripheral neuropathies, Neuroscience 244 (2013) 77–89, https://doi.org/10.1016/j.neuroscience.2013.03.050.

[10] G. Pignataro, B. Ziaco, A. Tortiglione, R. Gala, O. Cuomo, A. Vinciguerra, D. Lapi, T. Mastantuono, S. Anzilotti, L.D. D'Andrea, C. Pedone, G. di Renzo, L. Annunziato, M. Cataldi, Neuroprotective effect of VEGF-mimetic peptide QK in experimental brain ischemia induced in rat by middle cerebral artery occlusion, ACS Chem.

Neurosci. 6 (9) (2015) 1517–1525, https://doi.org/10.1021/acschemneuro.5b00175.
[11] L. De Rosa, R. Di Stasi, L.D. D'Andrea, Pro-angiogenic peptides in biomedicine, Arch. Biochem. Biophys. 660 (2018) 72–86, https://doi.org/10.1016/j.abb.2018.10.010.
[12] D. Diana, B. Ziaco, G. Colombo, G. Scarabelli, A. Romanelli, C. Pedone, R. Fattorusso, L.D. D'Andrea, Structural determinants of the unusual helix stability of a de novo engineered vascular endothelial growth factor (VEGF) mimicking peptide, Chemistry 14 (14) (2008) 4164–4166, https://doi.org/10.1002/chem.200800180.
[13] L. De Rosa, D. Diana, R. Di Stasi, A. Romanelli, M.F.M. Sciacca, D. Milardi, C. Isernia, R. Fattorusso, L.D. D'Andrea, Probing the helical stability in a VEGF-mimetic peptide, Bioorg. Chem. 116 (2021) 105379, https://doi.org/10.1016/j.bioorg.2021.105379.
[14] R. Aurora, G.D. Rose, Helix capping, Protein Sci. 7 (1) (1998) 21–38, https://doi.org/10.1002/pro.5560070103.
[15] B. Ziaco, D. Diana, D. Capasso, R. Palumbo, V. Celentano, R. Di Stasi, R. Fattorusso, L.D. D'Andrea, C-terminal truncation of vascular endothelial growth factor mimetic helical peptide preserves structural and receptor binding properties, Biochem Bioph Res Co 424 (2) (2012) 290–294, https://doi.org/10.1016/j.bbrc.2012.06.109.
[16] L. De Rosa, D. Diana, D. Capasso, R. Stefania, R. Di Stasi, R. Fattorusso, L. D. D'Andrea, Switching the N-capping region from all-L to all-D amino acids in a VEGF mimetic helical peptide, Molecules 27 (20) (2022) 6982, https://doi.org/10.3390/molecules27206982.
[17] A. Fontana, G. Fassina, C. Vita, D. Dalzoppo, M. Zamai, M. Zambonin, Correlation between sites of limited proteolysis and segmental mobility in thermolysin, Biochemistry 25 (8) (1986) 1847–1851, https://doi.org/10.1021/bi00356a001.
[18] R. Bucci, F. Foschi, C. Loro, E. Erba, M.L. Gelmi, S. Pellegrino, Fishing in the toolbox of cyclic turn mimics: a literature overview of the last decade, Eur. J. Org. Chem. 2021 (20) (2021) 2887–2900, https://doi.org/10.1002/ejoc.202100244.
[19] D. di Lorenzo, N. Bisi, R. Bucci, I. Ennen, L. Lo Presti, V. Dodero, R. Brandt, S. Ongeri, M.L. Gelmi, N. Tonali, Application of modular isoxazoline-β^{22}-amino acid-based peptidomimetics as chemical model systems for studying the tau misfolding, iScience 28 (4) (2025) 112272, https://doi.org/10.1016/j.isci.2025.112272.
[20] R. Bucci, A. Contini, F. Clerici, S. Pellegrino, M.L. Gelmi, From glucose to enantiopure morpholino β- amino acid: a new tool for stabilizing γ-turns in peptides, Org Chem Front 6 (7) (2019) 972–982, https://doi.org/10.1039/c8qo01116h.
[21] F. Vaghi, R. Bucci, F. Clerici, A. Contini, M.L. Gelmi, Non-natural 3-Arylmorpholino-β-amino acid as a PPII Helix inducer, Org. Lett. 22 (15) (2020) 6197–6202, https://doi.org/10.1021/acs.orglett.0c02331.
[22] J. Kong, S. Yu, Fourier transform infrared spectroscopic analysis of protein secondary structures, Acta Biochim. Biophys. Sin. Shanghai 39 (8) (2007) 549–559, https://doi.org/10.1111/j.1745-7270.2007.00320.x.
[23] D.S. Wishart, C.G. Bigam, A. Holm, R.S. Hodges, B.D. Sykes, 1H, 13C and 15N random coil NMR chemical shifts of the common amino acids. I. Investigations of nearest-neighbor effects, J. Biomol. NMR 5 (1) (1995) 67–81, https://doi.org/10.1007/BF00227471.
[24] D.S. Wishart, B.D. Sykes, F.M. Richards, The chemical shift index: a fast and simple method for the assignment of protein secondary structure through NMR spectroscopy, Biochemistry 31 (6) (1992) 1647–1651, https://doi.org/10.1021/bi00121a010.
[25] S. Pellegrino, N. Tonali, E. Erba, J. Kaffy, M. Taverna, A. Contini, M. Taylor, D. Allsop, M.L. Gelmi, S. Ongeri, beta-hairpin mimics containing a piperidine-pyrrolidine scaffold modulate the beta-amyloid aggregation process preserving the monomer species, Chem. Sci. 8 (2) (2017) 1295–1302, https://doi.org/10.1039/c6sc03176e.
[26] X. Li, J. Taechalertpaisarn, D. Xin, K. Burgess, Protein-protein interface mimicry by an oxazoline piperidine-2,4-dione, Org. Lett. 17 (3) (2015) 632–635, https://doi.org/10.1021/ol5036547.